Published in final edited form as:
Nano Lett. 2012 June 13; 12(6): 3322–3328. doi:10.1021/nl301529p.

Digital Switching of Local Arginine Density in a Genetically Encoded Self-Assembled Polypeptide Nanoparticle Controls Cellular Uptake

Sarah R. MacEwan[1] and **Ashutosh Chilkoti**[1,2,*]

[1]Department of Biomedical Engineering, Duke University, Box 90281, Durham, NC 27708

[2]Center for Biologically Inspired Materials and Material Systems, Duke University, Box 90271 Durham, NC 27708

Abstract

Cell-penetrating peptides (CPPs) are a class of molecules that enable efficient internalization of a wide variety of cargo in diverse cell types, making them desirable for delivery of anticancer drugs to solid tumors. For CPPs to be useful, it is important to be able to turn their function on in response to an external trigger that can be spatially localized *in vivo*. Here we describe an approach to turning on CPP function by modulation of the local density of arginine (Arg) residues by temperature-triggered micelle assembly of diblock copolymer elastin-like polypeptides (ELP_{BC}s). A greater than 8-fold increase in cellular uptake occurs when Arg residues are presented on the corona of ELP_{BC} micelles, as compared to the same ELP_{BC} at a temperature in which it is a soluble unimer. This approach is the first to demonstrate digital `off-on' control of CPP activity by an extrinsic thermal trigger in a clinically relevant temperature range by modulation of the interfacial density of Arg residues on the exterior of a nanoparticle.

Keywords

Cell-penetrating peptide; elastin-like polypeptide; micelle; self-assembly; cancer; drug delivery

Current approaches to cancer therapy rely heavily on chemotherapeutic agents whose cytotoxic actions are amplified in rapidly dividing cancer cells. Unfortunately, these agents also affect a subset of dividing healthy cells, resulting in toxic side effects that limit drug dose and ultimately hinder their therapeutic efficacy. Targeting systemically delivered drugs more precisely to the site of disease is a major goal in cancer chemotherapy so as to reduce off-target side effects and thereby increase their maximum tolerated dose and efficacy.

A number of active targeting strategies have been investigated that exploit unique features of tumors, such as overexpressed receptors,[1,2] upregulated enzymes,[3,4] depressed pH,[5,6] and hypoxia,[7,8] to enhance the systemic delivery of drug carriers to tumors. These approaches, however, are limited by several factors. First, overexpressed receptors or other cell surface proteins, although present at higher density in tumors, are also expressed by healthy cells, which leads to off-target accumulation and systemic toxicity. Second, many “tumor specific” features such as pH, hypoxia, and receptor expression exhibit great heterogeneity between different types of solid tumors, so that a strategy that seeks to exploit these features

*To whom correspondence should be addressed. chilkoti@duke.edu.

SUPPORTING INFORMATION. Experimental methods and detailed description of ELP_{BC} design are provided. This material is available and free of charge via the Internet at http://pubs.acs.org.

for targeted drug delivery is often applicable only to a narrow and specific subset of tumors.[9] Third, even within a single tumor type, there is great heterogeneity in these features between patients.[10–13]

In contrast, cell-penetrating peptides (CPPs) are an attractive –and conceptually orthogonal– targeting approach for drug delivery because they do not rely on unique features of tumors to achieve efficient cellular uptake.[14–17] These short peptides, such as TAT,[18] penetratin,[14] and oligoarginine[19] achieve internalization by mechanisms that are believed to be initiated by the electrostatic interaction and hydrogen bonding between a CPP and the phospholipid and proteoglycan components of cell membranes.[20,21] These putative interactions with ubiquitous components of the cell membrane enable CPPs to exhibit cellular uptake in a variety of cell lines.[16,17] CPPs also enable efficient uptake of attached cargo, as CPPs conjugated to proteins,[22] DNA,[23] liposomes,[24] and micelles[25] lead to efficient internalization of these diverse cargo. CPPs thus provide an exciting opportunity to create functionalized drug carriers capable of achieving cellular uptake in a wide range of cancer types.

Unfortunately, their complete lack of cellular specificity is problematic, as systemically delivered CPPs can be taken up in a number of organs within the body.[26,27] A `universal' tumor targeting system would thus combine the specificity of receptor-mediated targeting with the ubiquity and robustness of CPPs. This study focuses on solving this dilemma by the *in situ* triggered assembly of a CPP-presenting nanoparticle solely within a tumor. This approach builds upon the observation that oligoarginine CPPs display a strong cutoff effect in their cell penetration ability; below a threshold of six consecutive arginine (Arg) residues in the CPP, little internalization is observed, while above this threshold of Arg residues there is significant cell uptake.[19] We hypothesized that it is not the absolute number of Arg residues, but instead the local Arg density that is responsible for this threshold effect in cell uptake. This hypothesis then suggests that triggered micelle assembly of a diblock copolymer, with less than six Arg residues on its hydrophilic terminus, should provide a system that exhibits digital `off-on' cellular uptake because of the large difference in the local Arg density between the unimer and the micelle.

To create a targeted system with tumor-specific assembly of a functional CPP, we chose heat as the trigger and thermally responsive elastin-like polypeptides (ELPs) as the actuator to modulate the local density of Arg residues by an external thermal stimulus. Heat is an interesting trigger for targeted drug delivery because focused mild hyperthermia –wherein a specific region of the body is heated to a maximum *in vivo* temperature of approximately 42 °C– can be carried out in a clinical setting using microwaves,[28] radio-frequency,[29] or ultrasound.[30] Mild hyperthermia is of particular interest in oncology because compared to surrounding normal tissue, tumors have poor heat exchange properties because of their tortuous vasculature and low blood flow rates,[31,32] so that mild hyperthermia using an external applicator can be confined to solid tumors.[33]

We chose ELPs as the actuator to build a digital `off-on' switch of CPP activity because ELPs are peptide polymers[34] that exhibit lower critical solution temperature (LCST) phase transition behavior, such that below their LCST, or inverse transition temperature (T_t), they exist as soluble unimers, while above their T_t they coacervate into insoluble micron-size aggregates.[35] Diblock copolymer ELPs (ELP_{BC}s), composed of hydrophobic and hydrophilic ELP segments, are capable of temperature-triggered micelle assembly.[36–38] Upon thermally triggered selective desolvation of the hydrophobic segment, the amphiphilic ELP_{BC}s self-assemble into spherical micelles with a core consisting of the hydrophobic segment and a corona composed of the hydrophilic segment.

To exploit temperature-triggered micelle assembly of ELP_{BC}s to modulate the local Arg density, ELP_{BC}s were recombinantly designed to incorporate five Arg residues –below the threshold necessary for efficient cell uptake– at the terminus of the hydrophilic block (Arg_5-ELP_{BC}) (Figure 1A). Below their critical micelle temperature (CMT), we show that Arg_5-ELP_{BC}s exist as soluble unimers, whose interfacial Arg density is below the threshold necessary for cell uptake, preventing efficient cellular internalization in this `off state'. Above the CMT Arg_5-ELP_{BC}s self-assemble into spherical micelles that display an increased interfacial density of Arg residues on the hydrated surface of the micelle corona. We hypothesize that this dramatic increase in the local interfacial density of Arg residues exceeds the threshold necessary for uptake leading to efficient cellular internalization of the micelles in this `on state' (Figure 1B). We specifically chose a CMT in the range of 39–42 °C, which is typical of temperatures achieved with mild clinical hyperthermia.[39,40] The established clinical use of externally applied mild hyperthermia as adjuvant treatment for chemotherapy or external beam irradiation makes this approach practical to translate to the clinic.[40]

To achieve mild hyperthermia-triggered micelle assembly, the sequence, molecular weight (MW), and ratio of the hydrophobic and hydrophilic segments of the ELP_{BC} have to be precisely tuned to ensure that ELP_{BC}s are soluble unimers at 37 °C and that temperature-triggered micelle assembly occurs between 39 and 42 °C. The design of an ELP_{BC} with a specified CMT in such a narrow temperature range is not trivial for two reasons. First, although the T_t of a single segment ELP can be predicted with precision as a function of length and concentration for a given composition,[41] the CMT of an ELP_{BC} is difficult to predict *a priori* from the T_t of its constituent blocks due to the interactions between these blocks.[38] The CMT of the ELP_{BC} is also influenced by the addition of functional peptide sequences at the ELP_{BC}'s N- and C-terminus, due to the peptides' effect on the T_t of their adjacent block.

Our strategy for the synthesis of a suitable ELP_{BC} involved an iterative design cycle that required systematic adjustment in each design cycle of ELP_{BC} parameters including ELP sequence and block length. The design process is described in detail in the Supporting Information. After three iterative design cycles, which involved the synthesis and screening of approximately seven ELP_{BC}s, we identified one block copolymer that exhibited the desired CMT between 39 °C and 42 °C. This optimized ELP_{BC} was composed of a hydrophobic $(Val\text{-}Pro\text{-}Gly\text{-}Val\text{-}Gly)_{40}$ segment and a hydrophilic $(Val\text{-}Pro\text{-}Gly\text{-}X\text{-}Gly)_{60}$ segment, in which the guest residue X is Ala or Gly at a ratio of 1:1, and is referred to as Arg_5-ELP_{BC} in the remainder of this paper.

The thermal behavior of Arg_5-ELP_{BC} was characterized by temperature-programmed turbidimetry and dynamic light scattering (DLS) (Figure 2). The first transition temperature of the ELP_{BC} was observed at 38 °C as a modest increase in optical density, which is caused by its transition from unimer to micelle, and is hence defined as the CMT. The second transition temperature of the ELP_{BC}, indicated by a large increase in optical density, is consistent with a transition from micelles to micron-scale aggregates at approximately 56 °C. The hydrodynamic radius (R_h), measured by DLS as a function of temperature, agreed with the temperature-programmed turbidimetry, indicating a transition of ELP_{BC} from unimer (R_h <10 nm) to micelle (R_h ~20 nm) at 39 °C.

In addition to the Arg_5-ELP_{BC}, two control ELPs were synthesized. A control ELP_{BC} was designed with the same ELP_{BC} sequence as the Arg_5-ELP_{BC}, but without terminal Arg residues. This ELP_{BC} control served to deconvolute the role of micelle assembly from that of local Arg density on cellular uptake. Additionally, a single segment ELP was synthesized with the same composition as the hydrophilic domain of the ELP_{BC} and was functionalized

with five Arg residues at its C-terminus. This Arg_5-ELP control was designed to identify the role of Arg on cellular uptake, independent of micelle formation, as it was incapable of self-assembly and had a sufficiently high T_t, such that it existed as a soluble unimer at both 37 °C and 42 °C. All constructs contained an N-terminal cysteine residue on the opposite end of the C-terminal Arg_5 peptide, for conjugation of a maleimide derivative of Alexa Fluor 488. The MW and R_h of the three ELPs following fluorophore conjugation are listed in Table 1.

The cellular uptake of all three ELPs was examined *in vitro* with live cell confocal fluorescence microscopy. Human cervical cancer HeLa cells were incubated with Alexa 488- labeled ELP at 10 μM for 1 hour at 37 °C or 42 °C. There was no significant uptake by cells incubated with Arg_5-ELP_{BC}, ELP_{BC}, or Arg_5-ELP at 37 °C (Figure 3A–C), a temperature at which all constructs were soluble unimers. In agreement with previous studies,[19] the limited number of Arg residues on the Arg_5-ELP_{BC} unimer is below the threshold necessary for cellular internalization, thereby leading to minimal cell uptake in this `off state'. At 42 °C the self-assembled $Arg_5$-$ELP_{BC}$ micelle demonstrated significantly increased cellular uptake, as seen by punctate green fluorescence within the cell boundaries at this `on state' (Figure 3D). This internalized Arg_5-ELP_{BC} appeared to localize to the perinuclear space (Figure 3D – box). In contrast, the ELP_{BC} and Arg_5-ELP controls (Figure 3E–F) showed no increase in cellular uptake at 42 °C, as compared to 37 °C. These results support our hypothesis that it is not micelle assembly alone, or the presentation of Arg residues under hyperthermic conditions, that is responsible for the enhanced cellular uptake evident with the Arg_5-ELP_{BC} micelles. Cellular uptake thus requires the high –local– interfacial Arg density on the corona of the self-assembled Arg_5-ELP_{BC} micelle.

Live-cell flow cytometry was performed at different times post-incubation, to quantify the effect of enhanced Arg density on cellular uptake. Over the course of one hour at 42 °C, cells exhibited increasing cellular fluorescence when incubated with Arg_5-ELP_{BC}s, which display a high interfacial Arg density on the corona of their self-assembled micelles (Figure 4A). A minimal increase in cellular fluorescence was observed at 37 °C when cells were incubated with Arg_5-ELP_{BC}, which exists as a soluble unimer at 37 °C. Cellular fluorescence was low and approximately invariant over the course of one hour at 37 °C and 42 °C for ELP_{BC} (Figure 4B) and Arg_5-ELP (Figure 4C) controls. This data clearly shows that there was a dramatic, approximately 8-fold, difference in cellular uptake between 37 °C and 42 °C for Arg_5-ELP_{BC} as compared to either ELP_{BC} or Arg_5-ELP controls at all time points.

The fold-increase in uptake in the `on state' versus `off state' was calculated as the ratio of mean fluorescence intensity at 42 °C and 37 °C. This fold-increase in fluorescence serves as an *in vitro* metric to predict targeted cellular uptake by cells within a heated tumor compared to the cellular uptake in off-target tissues that are at physiological temperature. This metric, as well as the overall cellular uptake, is important to characterize the ability of Arg_5-ELP_{BC} to achieve sufficient uptake at the heated disease site while minimizing uptake at off-target tissues. Cells incubated with Arg_5-ELP_{BC} demonstrated a greater than 8-fold maximum increase in fluorescence at 42 °C, compared to 37 °C, after approximately 30 minutes of incubation (Figure 4A – black line). Furthermore, the maximal fold-increase in uptake between 42 °C and 37 °C is achieved within the standard one hour duration of mild clinical hyperthermia.[39]

To examine the utility of thermally triggered uptake of Arg_5-ELP_{BC}s across cell types, we quantified cellular internalization in two different tumor cell lines –HeLa (human cervical cancer) and MCF7 (human breast cancer)– as well as primary human umbilical vein endothelial cells (HUVECs), because endothelial cells in the tumor vasculature are the first cells that Arg_5-ELP_{BC}s will encounter when they are self-assembled into micelles as they

circulate through a heated tumor. Arg_5-ELP_{BC} showed a significantly greater fold-increase in cellular fluorescence between 42 °C and 37 °C, as compared to ELP_{BC} or Arg_5-ELP controls, in all three cell lines, though the effect in HUVECs was more modest (Figure 5). This suggests that uptake in the tumor vasculature is likely to only be modestly enhanced, with the major effect of increased uptake likely to be observed in tumor cells.

We next investigated the mechanism of cellular uptake. Although the exact mechanism of CPP-mediated cellular uptake is yet to be precisely and unequivocally elucidated, and is likely to depend upon the appended cargo, nanoparticles functionalized with Arg-rich CPPs have largely been shown to preferentially utilize endocytosis pathways other than clathrin-mediated endocytosis.[42,43] This is in contrast to carriers that utilize receptor-ligand interactions for cell uptake, which typically lead to clathrin-mediated endocytosis. To investigate the mechanism of uptake of ELP constructs, HeLa cells were co-incubated at 42 °C with ELP and dansylcadaverine, genistein, or amiloride, to inhibit clathrin-dependent endocytosis, caveolae-dependent endocytosis, or macropinocytosis, respectively (Figure 6A). After one hour, cells were analyzed by flow cytometry.

Cellular fluorescence in the presence of endocytosis inhibitors was normalized to the fluorescence of cells treated with the same ELP in the absence of that inhibitor. Dansylcadaverine had little effect on the cellular internalization of Arg_5-ELP_{BC}, ELP_{BC}, or Arg_5-ELP, suggesting that clathrin-mediated endocytosis is not the primary endocytosis pathway for these polypeptides. In contrast, genistein and amiloride decreased cellular internalization of Arg_5-ELP_{BC} by 57% and 80%, respectively, as compared to uptake in the absence of inhibitor. ELP_{BC} and Arg_5-ELP controls showed no significant change in cellular uptake in the presence of these inhibitors, with the exception of a decrease in uptake by 31% of Arg_5-ELP co-incubated with amiloride. These results agree with previous studies that carriers functionalized with oligoarginine CPPs exploit macropinocytosis as a predominant mechanism of cellular uptake.[44] Additionally, the enhanced effect of amiloride in decreasing cellular uptake of Arg_5-$ELP_{BC,}$ when compared with the Arg_5-ELP control, demonstrated the increase in macropinocytosis as the internalization mechanism with increasing density of Arg, similar to results observed for other Arg-decorated drug delivery vehicles.[44] However, Arg_5-ELP_{BC} appears to exploit more than one pathway of internalization, as a decrease in cellular uptake in the presence of genistein implicates caveolae-mediated endocytosis as a secondary mechanism for cellular uptake of Arg_5-ELP_{BC}.

These results were qualitatively confirmed by confocal microscopy of HeLa cells incubated with Arg_5-ELP_{BC} alone or in combination with dansylcadaverine, genistein, or amiloride at 42 °C (Figure 6B–E). Internalization of Arg_5-ELP_{BC} was observed in cells receiving no inhibitor treatment and uptake was not affected by the presence of dansylcadaverine. This was in contrast to cells incubated with genistein or amiloride, in which uptake was largely eliminated. These results confirmed that both caveolae-mediated endocytosis and macropinocytosis are important pathways for the uptake of Arg_5-ELP_{BC} micelles in their `on state'. These results are interesting as these mechanisms offer advantages for uptake of drug delivery vehicles, as they are less degradative routes of cellular entry compared to clathrin-mediated endocytosis. Studies have shown that caveolae-mediated endocytosis avoids intracellular lysosomal trafficking,[45] while macropinocytosis involves inherently leaky vesicles that permit some release of cargo, as well as intracellular routing that, in part, avoids fusion with lysosome compartments.[46] Together, these pathways provide routes of cellular entry that are likely to be less harmful to labile therapeutic cargo such as biologic drugs.

For CPPs to be useful for systemically delivered and tumor targeted drug delivery, their function must be precisely controlled outside of the disease site. Several approaches to this

challenge have involved the unmasking of CPPs by removal of stealth polymers that coat the CPP,[24,25,47,48] dissociation of CPPs from anionic inhibitors,[49,50] or triggered presentation of CPPs beyond a stealth coating using molecular actuator tethers.[51] All of these approaches depend on triggers intrinsic to solid tumors, such as pH[52] or enzymes,[53] to achieve CPP activation. These methods for controlling CPP function provide useful alternatives to traditional active targeting, but may be limited by several factors including their reliance on intrinsic tumor triggers, which can be heterogeneous across tumor type, and the irreversibility of CPP activation, which can result in off-target accumulation if the activated CPP-functionalized carrier leaks out of the tumor.

The approach presented here has the potential to surmount these limitations by exploiting an extrinsic thermal trigger to control CPP activation by the interfacial –local– modulation of Arg density on the exterior of a self-assembled nanoparticle. This approach circumvents the heterogeneity of tumor phenotypes by avoiding the use of intrinsic tumor triggers (such as pH or protease levels) while providing a digital `off-on' switch for CPP activation by focused mild hyperthermia in a narrow, clinically relevant, temperature window. The digital switching of Arg density also biases uptake towards endocytic pathways that avoid lysosomal accumulation and thereby prevent premature degradation of labile cargo. Together, these properties provide a new nanoscale approach to harness the power of CPPs for targeted drug delivery.

Supplementary Material

Refer to Web version on PubMed Central for supplementary material.

Acknowledgments

This work was supported by NIH grant R01EB007205 (A.C.) and by the NSF through the Research Triangle MRSEC (NSF DMR-11-21107).

REFERENCES

(1). Peer D, Karp JM, Hong S, Farokhzad OC, Margalit R, Langer R. Nature nanotechnology. 2007; 2:751–760.

(2). Yu B, Tai HC, Xue W, Lee LJ, Lee RJ. Molecular membrane biology. 2010; 27:286–298. [PubMed: 21028937]

(3). Vartak DG, Gemeinhart RA. J Drug Target. 2007; 15:1–20. [PubMed: 17365270]

(4). MacEwan SR, Callahan DJ, Chilkoti A. Nanomedicine. 2010; 5:793–806. [PubMed: 20662649]

(5). Lee ES, Gao Z, Bae YH. J Control Release. 2008; 132:164–170. [PubMed: 18571265]

(6). Manchun S, Dass CR, Sriamornsak P. Life sciences. 2012; 90:381–387. [PubMed: 22326503]

(7). Kizaka-Kondoh S, Inoue M, Harada H, Hiraoka M. Cancer Sci. 2003; 94:1021–1028. [PubMed: 14662015]

(8). Wilson WR, Hay MP. Nat Rev Cancer. 2011; 11:393–410. [PubMed: 21606941]

(9). Parker N, Turk MJ, Westrick E, Lewis JD, Low PS, Leamon CP. Anal Biochem. 2005; 338:284–293. [PubMed: 15745749]

(10). Muss HB, Thor AD, Berry DA, Kute T, Liu ET, Koerner F, Cirrincione CT, Budman DR, Wood WC, Barcos M, et al. N Engl J Med. 1994; 330:1260–1266. [PubMed: 7908410]

(11). Fink-Retter A, Gschwantler-Kaulich D, Hudelist G, Mueller R, Kubista E, Czerwenka K, Singer CF. Oncol Rep. 2007; 18:299–304. [PubMed: 17611648]

(12). Taniguchi K, Okami J, Kodama K, Higashiyama M, Kato K. Cancer Sci. 2008; 99:929–935. [PubMed: 18325048]

(13). Dexter DL, Leith JT. J Clin Oncol. 1986; 4:244–257. [PubMed: 3944607]

(14). Derossi D, Calvet S, Trembleau A, Brunissen A, Chassaing G, Prochiantz A. J Biol Chem. 1996; 271:18188–18193. [PubMed: 8663410]

(15). Kerkis A, Hayashi MA, Yamane T, Kerkis I. IUBMB life. 2006; 58:7–13. [PubMed: 16540427]

(16). Mueller J, Kretzschmar I, Volkmer R, Boisguerin P. Bioconjug Chem. 2008; 19:2363–2374. [PubMed: 19053306]

(17). Olson ES, Aguilera TA, Jiang T, Ellies LG, Nguyen QT, Wong EH, Gross LA, Tsien RY. Integr Biol (Camb). 2009; 1:382–393. [PubMed: 20023745]

(18). Frankel AD, Pabo CO. Cell. 1988; 55:1189–1193. [PubMed: 2849510]

(19). Wender PA, Mitchell DJ, Pattabiraman K, Pelkey ET, Steinman L, Rothbard JB. Proc Natl Acad Sci U S A. 2000; 97:13003–13008. [PubMed: 11087855]

(20). Rothbard JB, Jessop TC, Lewis RS, Murray BA, Wender PA. J Am Chem Soc. 2004; 126:9506–9507. [PubMed: 15291531]

(21). Nakase I, Tadokoro A, Kawabata N, Takeuchi T, Katoh H, Hiramoto K, Negishi M, Nomizu M, Sugiura Y, Futaki S. Biochemistry. 2007; 46:492–501. [PubMed: 17209559]

(22). Wadia JS, Dowdy SF. Adv Drug Deliv Rev. 2005; 57:579–596. [PubMed: 15722165]

(23). Astriab-Fisher A, Sergueev D, Fisher M, Shaw BR, Juliano RL. Pharm Res. 2002; 19:744–754. [PubMed: 12134943]

(24). Kale AA, Torchilin VP. J Drug Target. 2007; 15:538–545. [PubMed: 17671900]

(25). Sethuraman VA, Lee MC, Bae YH. Pharm Res. 2008; 25:657–666. [PubMed: 17999164]

(26). Aguilera TA, Olson ES, Timmers MM, Jiang T, Tsien RY. Integr Biol (Camb). 2009; 1:371–381. [PubMed: 20023744]

(27). Miyaji Y, Walter S, Chen L, Kurihara A, Ishizuka T, Saito M, Kawai K, Okazaki O. Drug metabolism and disposition: the biological fate of chemicals. 2011; 39:1946–1953. [PubMed: 21712433]

(28). Jones E, Thrall D, Dewhirst MW, Vujaskovic Z. Int J Hyperthermia. 2006; 22:247–253. [PubMed: 16754346]

(29). James JR, Gao Y, Soon VC, Topper SM, Babsky A, Bansal N. Int J Hyperthermia. 2010; 26:79–90. [PubMed: 20100055]

(30). O'Neill BE, Li KC. Int J Hyperthermia. 2008; 24:506–520. [PubMed: 18608574]

(31). Alpard SK, Vertrees RA, Tao W, Deyo DJ, Brunston RL Jr. Zwischenberger JB. Perfusion. 1996; 11:425–435. [PubMed: 8971942]

(32). Thrall DE. Radiation and environmental biophysics. 1980; 17:229–232. [PubMed: 7443978]

(33). Ranjan A, Jacobs GC, Woods DL, Negussie AH, Partanen A, Yarmolenko PS, Gacchina CE, Sharma KV, Frenkel V, Wood BJ, Dreher MR. J Control Release. 2012; 158:487–494. [PubMed: 22210162]

(34). Tatham AS, Shewry PR. Trends Biochem Sci. 2000; 25:567–571. [PubMed: 11084370]

(35). Urry DW. J. Phys. Chem. B. 1997; 101:11007–11028.

(36). Lee TAT, Cooper A, Apkarian RP, Conticello VP. Adv. Mater. 2000; 12:1105–1110.

(37). Wright ER, Conticello VP. Adv Drug Deliv Rev. 2002; 54:1057–1073. [PubMed: 12384307]

(38). Dreher MR, Simnick AJ, Fischer K, Smith RJ, Patel A, Schmidt M, Chilkoti A. J Am Chem Soc. 2008; 130:687–694. [PubMed: 18085778]

(39). Roemer RB. Annu Rev Biomed Eng. 1999; 1:347–376. [PubMed: 11701493]

(40). Falk MH, Issels RD. Int J Hyperthermia. 2001; 17:1–18. [PubMed: 11212876]

(41). Meyer DE, Chilkoti A. Biomacromolecules. 2004; 5:846–851. [PubMed: 15132671]

(42). Fittipaldi A, Ferrari A, Zoppe M, Arcangeli C, Pellegrini V, Beltram F, Giacca M. J Biol Chem. 2003; 278:34141–34149. [PubMed: 12773529]

(43). Jones SW, Christison R, Bundell K, Voyce CJ, Brockbank SM, Newham P, Lindsay MA. British journal of pharmacology. 2005; 145:1093–1102. [PubMed: 15937518]

(44). Khalil IA, Kogure K, Futaki S, Harashima H. J Biol Chem. 2006; 281:3544–3551. [PubMed: 16326716]

(45). Shin JS, Abraham SN. Science. 2001; 293:1447–1448. [PubMed: 11520975]

(46). Khalil IA, Kogure K, Akita H, Harashima H. Pharmacological reviews. 2006; 58:32–45. [PubMed: 16507881]

(47). Mok H, Bae KH, Ahn CH, Park TG. Langmuir. 2009; 25:1645–1650. [PubMed: 19117377]

(48). Sawant RM, Hurley JP, Salmaso S, Kale A, Tolcheva E, Levchenko TS, Torchilin VP. Bioconjug Chem. 2006; 17:943–949. [PubMed: 16848401]

(49). Goun EA, Shinde R, Dehnert KW, Adams-Bond A, Wender PA, Contag CH, Franc BL. Bioconjug Chem. 2006; 17:787–796. [PubMed: 16704219]

(50). Olson ES, Jiang T, Aguilera TA, Nguyen QT, Ellies LG, Scadeng M, Tsien RY. Proc Natl Acad Sci U S A. 2010; 107:4311–4316. [PubMed: 20160077]

(51). Lee ES, Gao Z, Kim D, Park K, Kwon IC, Bae YH. J Control Release. 2008; 129:228–236. [PubMed: 18539355]

(52). Cardone RA, Casavola V, Reshkin SJ. Nat Rev Cancer. 2005; 5:786–795. [PubMed: 16175178]

(53). Roy R, Yang J, Moses MA. J Clin Oncol. 2009; 27:5287–5297. [PubMed: 19738110]

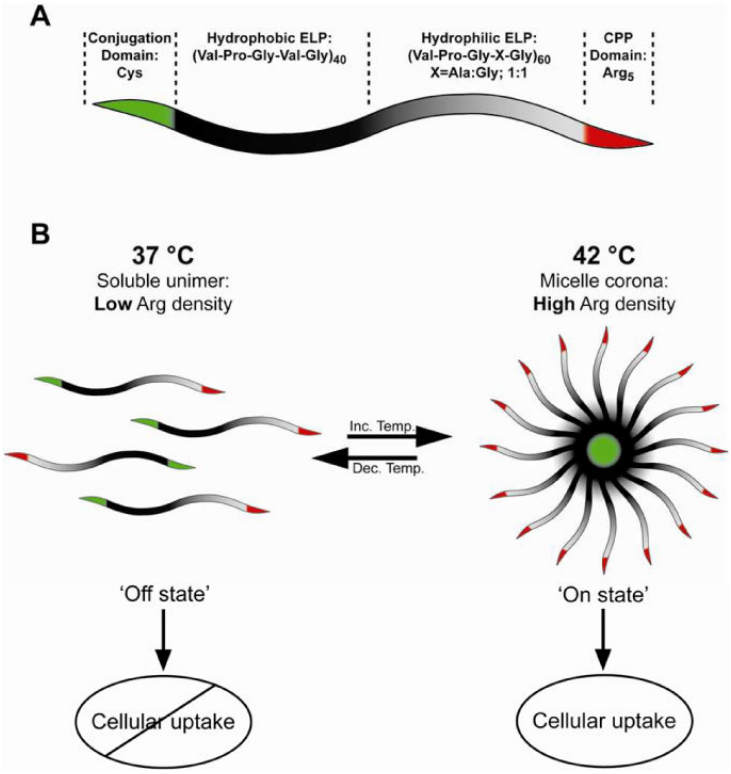

Figure 1.

(A) Controlled cellular uptake by modulation of local Arg density is achieved by temperature-triggered micelle assembly of a genetically encoded Arg_5-ELP_{BC}. (B) `Off state': At 37 °C, below the CMT, $Arg_5$-$ELP_{BC}$s exist as soluble unimers, whose limited number of Arg residues is below the threshold necessary for efficient cellular uptake. `On state': Above the CMT at 42 °C (a temperature that can be achieved with mild clinical hyperthermia) Arg_5-ELP_{BC}s assemble into spherical micelles. The high density of Arg decorating the micelle corona exceeds the threshold of Arg residues necessary for internalization, leading to cellular uptake of the micelles.

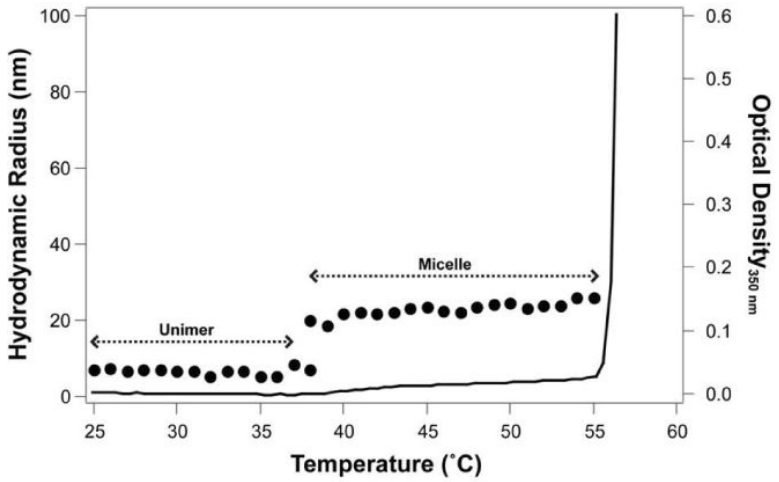

Figure 2.

Arg_5-ELP_{BC} was characterized by temperature-programmed turbidimetry and DLS. The optical density at 350 nm (black line) indicated that Arg_5-ELP_{BC}s existed as soluble unimers with a R_h of <10 nm as determined by DLS (dots) up to 39 °C. At 39 °C Arg_5-ELP_{BC}s self-assembled into micelles with a R_h of approximately 20 nm that persisted up to 56 °C. Above 56 °C, Arg_5-ELP_{BC} formed micron-size aggregates.

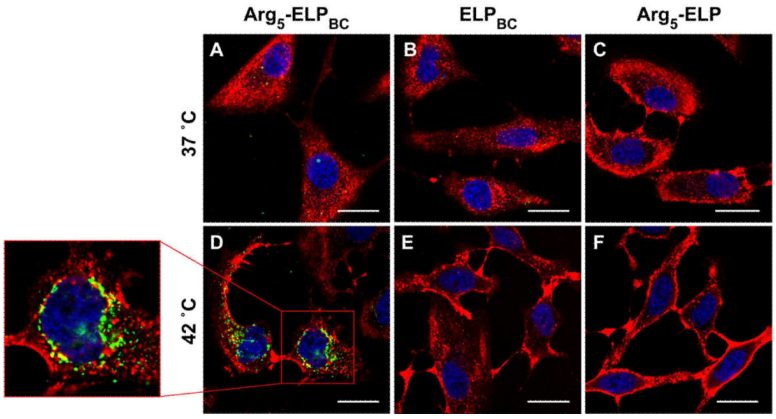

Figure 3.

Digital switching of cellular uptake by modulation of Arg density was investigated by live cell confocal microscopy. No significant cellular uptake was evident after incubation with Arg_5-ELP_{BC} (A), ELP_{BC} (B), or Arg_5-ELP (C) at 37 °C, a temperature at which all constructs existed as soluble unimers. At 42 °C temperature-triggered micelle assembly of Arg_5-ELP_{BC} increased the local density of Arg on the micelle corona, resulting in enhanced cellular uptake, evident as punctate green intracellular fluorescence (D). This internalized Arg_5-ELP_{BC} localized to the perinuclear space (D – box). No increase in cellular uptake was observed with the ELP_{BC} (E) or Arg_5-ELP (F) controls at 42 °C. Green: ELP; Red: cell membrane; Blue: cell nuclei; scale bars 25 μm.

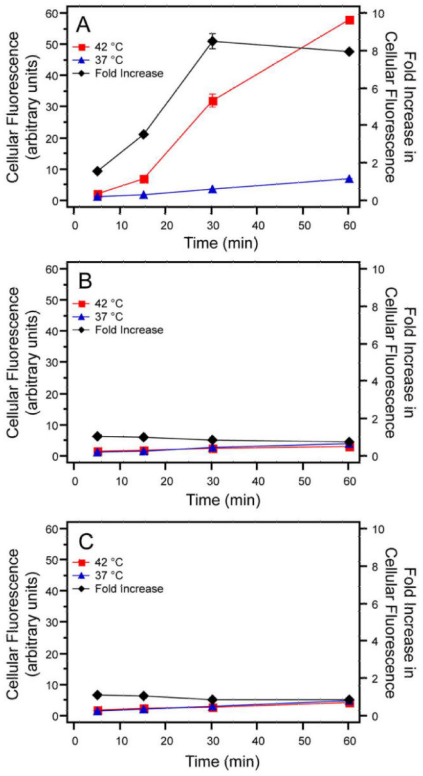

Figure 4.

Cellular uptake was quantified by measurement of fluorescence with live-cell flow cytometry. Fluorescence of cells incubated with Arg_5-ELP_{BC} at 42 °C increased significantly over the course of one hour, while those incubated at 37 °C showed little enhancement in fluorescence (A). ELP_{BC} (B) and Arg_5-ELP (C) controls showed minimal change in uptake over the course of an hour and showed little difference in uptake between 37 °C and 42 °C at each time point. The fold increase in cellular fluorescence (black line), calculated as the fluorescence at 42 °C divided by the fluorescence at 37 °C, reached approximately 8-fold for Arg_5-ELP_{BC} within one hour. Data represents the average of two replicates ± SEM.

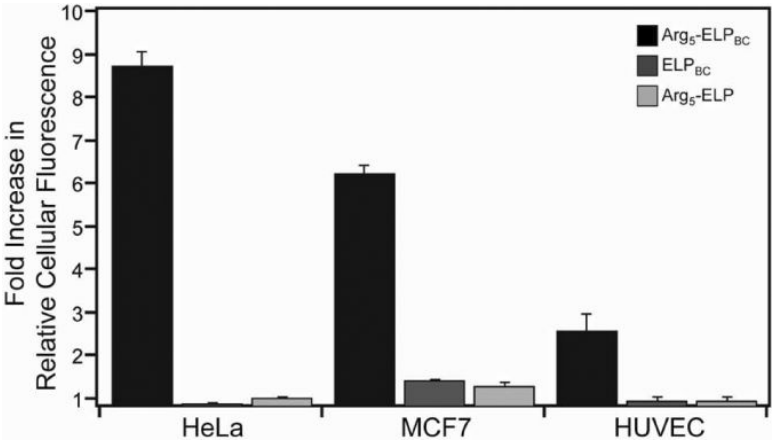

Figure 5.

Cellular uptake was quantified in three cell lines by live-cell flow cytometry. The fold-increase in fluorescence at 42 °C, as compared to 37 °C, was measured for HeLa cervical cancer cells, MCF7 breast cancer cells, and primary HUVECs. All cell lines demonstrated the effect of Arg density modulation by temperature-triggered micelle assembly in controlling cellular uptake, as the fold-increase in cellular fluorescence of Arg_5-ELP_{BC} was significantly greater than ELP_{BC} or Arg_5-ELP controls within each cell line. Data represents the average of 3 experiments ± SEM.

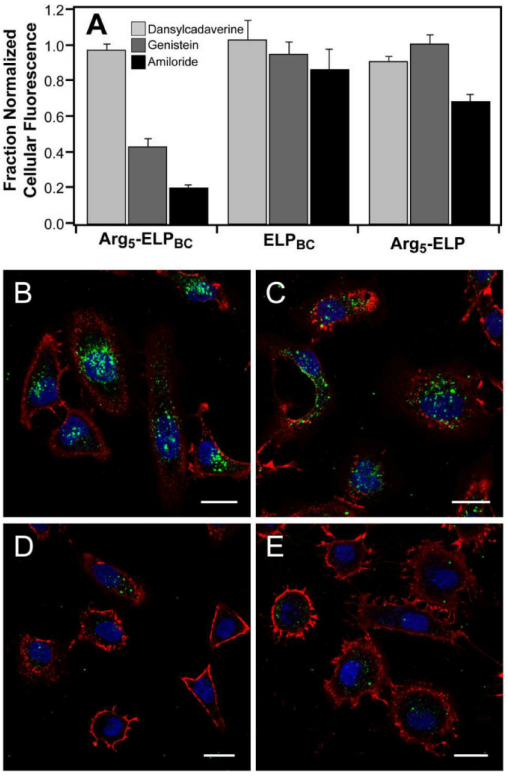

Figure 6.

The mechanism of cellular internalization was investigated by flow cytometry and confocal microscopy of cells co-incubated with ELP and endocytosis inhibitors at 42 °C. Cellular uptake, as measured by cellular fluorescence, significantly decreased for Arg_5-ELP_{BC} micelles co-incubated with genistein or amiloride, but not dansylcadaverine (A). This effect was more pronounced for Arg_5-ELP_{BC} as compared to ELP_{BC} or Arg_5-ELP controls. This suggests that caveolae-mediated endocytosis and macropinocytosis play important roles in the internalization of Arg_5-ELP_{BC}s in their micelle state. Confocal microscopy of cells incubated with Arg_5-ELP_{BC} micelles alone (B), or in combination with dansylcadaverine (C), genistein (D), or amiloride (E) support the conclusions drawn from flow cytometry. Data represents average of 3 experiments ± SEM. Green – ELP; Red – cell membrane; blue – cell nuclei; scale bars 25 μm. Signal from the ELP is shown as a maximum intensity projection, demonstrating cellular uptake throughout the volume of the cell.

Table 1

Characterization of Alexa 488-labeled ELP constructs.

Construct	ELP	C-terminal functionality	MW (kDa)	R_h (nm) 37 °C[1]	R_h (nm) 42 °C[1]
Arg_5-ELP_{BC}	$(Val\text{-}Pro\text{-}Gly\text{-}Val\text{-}Gly)_{40}$-$(Val\text{-}Pro\text{-}Gly\text{-}X\text{-}Gly)_{60}$ [X=Ala:Gly]	Arg_5	40.6	5.5 ± 0.1	21.0 ± 1.3
ELP_{BC}	$(Val\text{-}Pro\text{-}Gly\text{-}Val\text{-}Gly)_{40}$-$(Val\text{-}Pro\text{-}Gly\text{-}X\text{-}Gly)_{60}$ [X=Ala:Gly]	none	39.8	5.8 ± 0.2	20.5 ± 0.6
Arg_5-ELP	$(Val\text{-}Pro\text{-}Gly\text{-}X\text{-}Gly)_{100}$ [X=Ala:Gly]	Arg_5	39.2	5.4 ± 0.2	5.2 ± 0.1

[1] ELP at 10 μM in PBS. Data represents the average of 3 replicates ± SEM.